Proc. Natl. Acad. Sci. USA
Vol. 90, pp. 3745–3749, April 1993
Biochemistry

Thrombin-binding DNA aptamer forms a unimolecular quadruplex structure in solution

ROMÁN F. MACAYA*, PETER SCHULTZE*, FLINT W. SMITH*, JAMES A. ROE†, AND JULI FEIGON*‡

*Department of Chemistry and Biochemistry and Molecular Biology Institute, University of California, Los Angeles, CA 90024; and †Department of Chemistry and Biochemistry, Loyola Marymount University, Los Angeles, CA 90045

Communicated by Richard E. Dickerson, January 14, 1993 (received for review November 16, 1992)

ABSTRACT **We have used two-dimensional ^{1}H NMR spectroscopy to study the conformation of the thrombin-binding aptamer d(GGTTGGTGTGGTTGG) in solution. This is one of a series of thrombin-binding DNA aptamers with a consensus 15-base sequence that was recently isolated and shown to inhibit thrombin-catalyzed fibrin clot formation *in vitro* [Bock, L. C., Griffin, L. C., Latham, J. A., Vermaas, E. H. & Toole, J. J. (1992) *Nature (London)* 355, 564–566]. The oligonucleotide forms a unimolecular DNA quadruplex consisting of two G-quartets connected by two TT loops and one TGT loop. A potential T·T bp is formed between the two TT loops across the diagonal of the top G-quartet. Thus, all of the invariant bases in the consensus sequence are base-paired. This aptamer structure was determined by NMR and illustrates that this molecule forms a specific folded structure. Knowledge of this structure may be used in the further development of oligonucleotide-based thrombin inhibitors.**

The ability of nucleic acids to fold into a variety of different structures has been exploited in the development of techniques for the isolation of aptamers (1) which are DNA or RNA oligonucleotides that have been screened from a randomly generated population of sequences for their ability to bind a desired molecular target (2–4). The isolation process involves repeated cycles of selection for, and enrichment of, oligonucleotides with an affinity to a specific target, followed by amplification of these sequences using the PCR (5). Oligonucleotides with the selected characteristics—i.e., binding to a specific molecule—are finally identified through cloning and sequencing. The potential of these methods for the development of oligonucleotide-based therapeutics has recently been explored by their application in isolating oligonucleotide ligands that selectively inhibit the activity of a target protein. Selection of DNA aptamers that bind to thrombin and inhibit thrombin-catalyzed fibrin–clot formation *in vitro* (6) and more recently an RNA oligonucleotide that specifically inhibits cDNA synthesis by human immunodeficiency virus reverse transcriptase *in vitro* (7) have been reported.

Here we report two-dimensional NMR studies of the thrombin-binding aptamer d(GGTTGGTGTGGTTGG) (thrombin aptamer) that conforms to the consensus sequence d(GGtTGGN$_{2-5}$GGtTGG), where an uppercase letter indicates an invariant base, a lowercase letter indicates a base bias at that position, and there are usually three central N nucleotides (6). The oligonucleotide folds into a unimolecular quadruplex containing two G-quartets (8) linked by two TT loops at one end and a TGT loop at the other end. The invariant thymines in the TT loops are potentially base-paired across the top of one G-quartet. This aptamer structure was determined by NMR techniques and illustrates that this molecule forms a specific folded structure. Knowledge of this structure should be useful in the further development of oligonucleotide-based therapeutics or as a starting point for small-molecule drug design.

The publication costs of this article were defrayed in part by page charge payment. This article must therefore be hereby marked "*advertisement*" in accordance with 18 U.S.C. §1734 solely to indicate this fact.

MATERIALS AND METHODS

Sample Preparation. The DNA oligonucleotides were synthesized and purified; NMR samples were prepared as described (9, 10). The DNA oligonucleotides used were d(G^{1}G^{2}T^{3}T^{4}G^{5}G^{6}T^{7}G^{8}T^{9}G^{10}G^{11}T^{12}T^{13}G^{14}G^{15}) (thrombin aptamer) and the inosine, adenine, and deoxyuracil derivatives d(GITTGGTGTGGTTGG) (sequence I2), d(GGTTGITGTGGTTGG) (sequence I6), d(GGTTGGTITGGTTGG) (sequence I8), d(GGTTGGTGTGITTGG) (sequence I11), d(GGATGGTGTGGTTGG) (sequence A3), and d(GGTUGGTGTGGTTGG) (sequence U4).

NMR Spectroscopy. ^{1}H NMR spectra were obtained at 500 MHz on a General Electric GN500 spectrometer. One-dimensional spectra in H_2O were acquired using a 1$\bar{1}$ spin-echo pulse sequence (11). Nuclear Overhauser effect (NOE) spectroscopy (NOESY) spectra in H_2O were acquired in the hypercomplex phase-sensitive mode (12) with the standard pulse sequence (13) and the last pulse replaced by a 1$\bar{1}$ spin-echo pulse sequence (11). Phase-sensitive NOESY spectra in ^2H_2O were acquired with presaturation of the residual H_2O peak during the recycle delay. Purged correlated spectroscopy (P.COSY) spectra were acquired with a flip angle mixing pulse of 90° (14). Homonuclear Hartmann–Hahn (HOHAHA) experiments were run with 50–60 MLEV17 cycles (15). One-dimensional spectra were processed with the General Electric NMR software (GEM1). Two-dimensional spectra were processed on a Silicon Graphics 4D/25 Iris work station using the program FTNMR and FELIX (Hare Research, Seattle). Acquisition and processing parameters are given in the figure legends.

Assignments. Assignments of the deoxyribose spin systems and identification of base proton resonances were made from NOESY (13), P.COSY (14), and HOHAHA (15) spectra by using standard methods (10, 16). Sequential assignment of the nucleotides (10, 16) was complicated by breaks in the sequential connectivities after T^4, T^7, T^9, and T^{13} due to the presence of *syn*-guanine nt and loops (see Fig. 3*A*). Base-specific assignments were confirmed by comparison to spectra obtained with inosine-, uracil-, and adenine-substituted oligonucleotides, as discussed below. Once the nonexchangeable base proton resonances were assigned, the exchangeable imino and amino resonances were assigned by using NOE crosspeaks observed in NOESY spectra in H_2O. These NOEs included intraquartet GH8–G-amino–G-imino crosspeaks (9) as well as crosspeaks between resonances in the G-quartets and the thymine nucleotides. Assignments

Abbreviations: NOE, nuclear Overhauser effect; NOESY, NOE spectroscopy; P.COSY, purged correlated spectroscopy; HOHAHA, homonuclear Hartmann–Hahn; DSC, differential scanning calorimetry.

‡To whom reprint requests should be addressed.

were obtained for all exchangeable and nonexchangeable resonances of the thrombin aptamer, except for the T^3 and T^{12} imino resonances and some H5′,H5″ resonances and will be presented in detail elsewhere. The assignments were confirmed in a ^{31}P-^1H heteroCOSY spectrum (unpublished work).

Model Structure Determination. The 248 distance constraints derived from NOE peak intensities and constraints for 16 H-bonds forming the G-quartets as well as two H-bonds for the T^4·T^{13} bp as well as 80 dihedral bond-angle constraints were used for metric matrix distance substructure embedding with X-PLOR version 3.0 (17), followed by template fitting and subsequent regularization by simulated annealing and energy minimization. Out of 20 structures thus obtained the six with the lowest overall energies were subjected to relaxation matrix refinement, using the integrated peak intensities for four NOESY experiments (18) in ^2H_2O at mixing times of 50, 100, 150, 250 ms. The model shown in Fig. 6 has the lowest *R* factor between calculated and observed NOE peak integrals among those six structures. Details of the refined structures will be presented elsewhere (unpublished work).

Differential Scanning Calorimetry (DSC). The DSC was done with a Micro-Cal 2 differential scanning calorimeter. The scan rate was 1°C per min, and samples were scanned from 15 to 90°C under 2 atmospheres of N_2. Concentrations of aptamer were 0.06–0.8 mM and were made from dilution of stock solutions. The melting temperature, t_m, was defined as the temperature at peak maximum.

RESULTS AND DISCUSSION

Imino Proton Spectra Indicate a G-Quadruplex Structure. The one-dimensional ^1H NMR spectrum of the exchangeable resonances of the thrombin aptamer in the approximate salt conditions used in the selection buffer (140 mM NaCl/5 mM KCl/1 mM $CaCl_2$/1 mM $MgCl_2$) (6) is shown in Fig. 1. The eight hydrogen-bonded G-imino proton resonances observed between 11.8 and 12.3 ppm are consistent with the formation of G-quartets (9, 19–21), and this was confirmed as discussed below. NOESY spectra of this molecule in H_2O (data not shown) show NOE crosspeaks characteristic of G-quartet structures, including crosspeaks between G-imino protons, slowly exchanging G-amino protons, and GH8 resonances (9). Four-stranded structures containing G-quartets have been proposed for a variety of synthetic and naturally occurring G-rich (oligo)nucleotides (for review, see ref. 8).

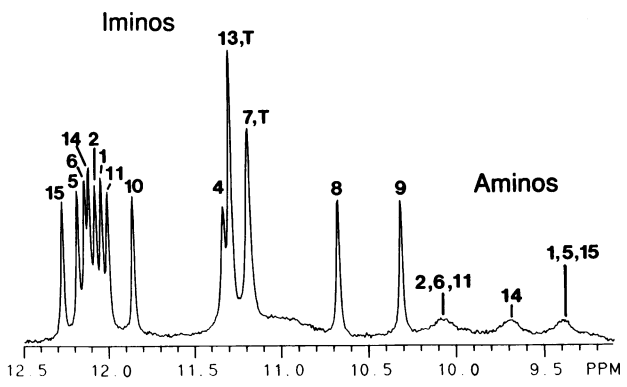

FIG. 1. (*A*) 500 MHz one-dimensional ^1H NMR spectrum of the imino and hydrogen-bonded amino protons of d($G^1G^2T^3T^4G^5G^6T^7$-$G^8T^9G^{10}G^{11}T^{12}T^{13}G^{14}G^{15}$) (thrombin aptamer) in 90% H_2O/10% ^2H_2O/140 mM NaCl/5 mM KCl/1 mM $CaCl_2$/1 mM $MgCl_2$, pH 6.1/1.0 mM DNA strand at 1°C. Assignments of imino and hydrogen-bonded amino resonances are indicated on the spectrum. The corresponding non-hydrogen-bonded aminos are observed between 6.2 and 6.9 ppm; amino resonances from the non-base-paired G^8 are at 5.80 ppm.

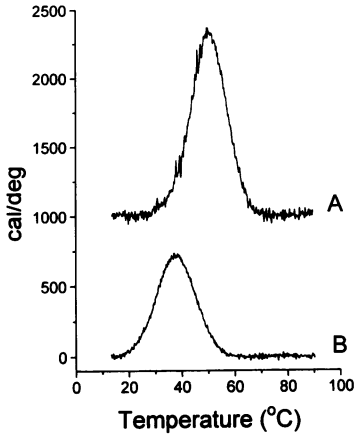

FIG. 2. DSC of thrombin aptamer in 100 mM potassium phosphate, pH 6.1/0.5 mM DNA (*A*) and 20 mM Tris acetate, pH 7.4/140 mM NaCl/5 mM KCl/1 mM $CaCl_2$/1 mM $MgCl_2$, 0.8 mM DNA (*B*). Starting values for the vertical scale are arbitrary.

The Aptamer Structure Is Stabilized by K^+. Fig. 2 shows the results of DSC on the sample in the selection buffer and in 100 mM potassium phosphate. A single melting transition is observed, with a t_m of 38°C in the selection buffer, and a melting enthalpy (ΔH_d) of 11 ± 0.6 kcal/mol. The t_m increases to 51°C for the sample in 100 mM potassium phosphate, with a ΔH_d of 22 ± 0.4 kcal/mol. The increase in both t_m and ΔH_d

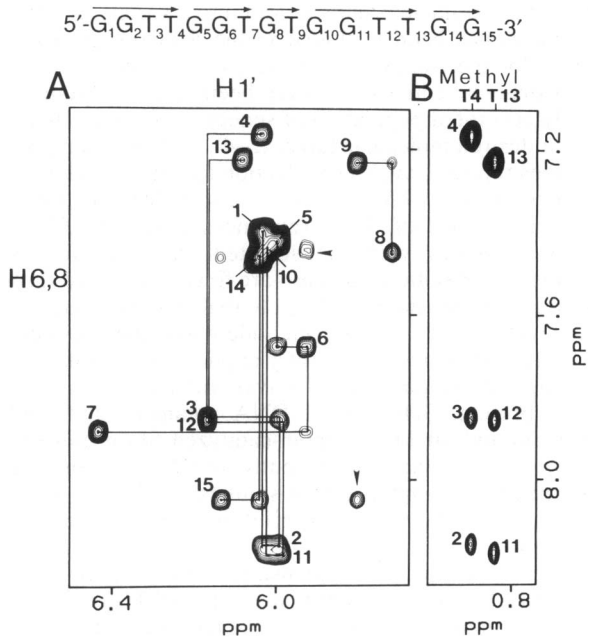

FIG. 3. Regions of NOESY spectrum (τ_m = 250 msec) of thrombin aptamer in 110 mM KCl, pH 6.1/2.3 mM DNA strand in ^2H_2O at 20°C showing the aromatic-H1′ (*A*) and aromatic-T^4 and T^{13} methyl (*B*) crosspeaks. (*A*) Sequential base-H1′ connectivities (9, 16) are indicated by solid lines in the spectrum and on the sequence above. Sequential base-H1′ connectivities are observed for G^1–T^4, G^5–T^7, G^8–T^9, G^{10}–T^{13}, and G^{14}–G^{15}. Base-H1′ connectivities for T^3–T^4 and T^{12}–T^{13} are very weak and can only be seen at low contour levels. Arrowheads point to nonsequential NOEs between T^9H1′ and G^{15}H8 and between G^6H1′ and G^8H8. (*B*) Crosspeaks are observed from T^4 and T^{13} methyls to G^2H8 and G^{11}H8, respectively, in the adjacent quartet, as well as to the neighboring T^3H6 and T^{12}H6. NOESY spectra in ^2H_2O were acquired with a spectral width of 5000 Hz, 2048 complex points in t_2, 64 scans per t_1 value, and 280–300 t_1 values, and processed as described (9, 10).

in the potassium buffer indicates that this buffer stabilizes the structure of the aptamer as compared to the selection buffer. The one-dimensional imino-proton spectrum as well as two-dimensional NMR spectra of the thrombin aptamer at low temperature in 110 mM KCl were essentially identical to those in the selection buffer (data not shown). However, as expected from the DSC results, NMR samples of the aptamer in the selection buffer have lower t_m values in the selection buffer than in KCl solution. K^+ stabilizes G-quadruplexes relative to Na^+, whereas most divalent cations are destabilizing (8, 22–25). Because of the higher stability of the thrombin aptamer structure in KCl, most NMR spectra were obtained on samples in 110 mM KCl solution.

Guanine Nucleotides Are 5′-*syn*–*anti*-3′ Along Each Strand of the Quadruplex. A portion of the NOESY spectrum of the thrombin aptamer containing the crosspeaks between the base and H1′ protons is shown in Fig. 3*A*. The intensities of NOESY crosspeaks between the base and sugar H1′ resonances of the thrombin aptamer indicate that there are four *syn*-G (G^1,G^5,G^{10}, and G^{14}) and five *anti*-G nt. Each of the four *syn*-G nt has sequential connectivities to a 3′ neighboring *anti*-G. The crosspeak patterns indicate that they are 5′-G-*syn*–G-anti-3′ along each strand of the two quartets (9), as observed for other folded G-quadruplex structures (9, 19, 26, 27). There are no sequential connectivities between the last (3′) thymine in each loop (T^4, T^9, and T^{13}) and the following *syn*-G. All of the thymine nt are *anti*.

Confirmation of G-Quartet Structure and Identification of Bases Within the G-Quartets and Loops. The sequential connectivities observed in NOESY spectra between 5′ *syn*-G and 3′ *anti*-G nt and connectivities to neighboring thymine nt allowed identification of partial runs of guanines and thymines along the strand but did not allow unambiguous identification of location in the strand or relative orientation of the guanines in the G-quartets. To confirm the assignments and orientation of guanines in the G-quartets, NOESY spectra were obtained on several inosine-, adenine-, and uracil-containing derivatives of the thrombin aptamer. All derivatives folded into the same general structure as the parent thrombin aptamer, as determined from NOESY spectra (Fig. 4, 5A and spectra not shown). However, the stability of all derivatives except sequences U4 and I8 was lower than that of the thrombin aptamer, as judged from NMR temperature studies. Fig. 4*A* shows the region of a NOESY spectrum of sequence I2 containing the aromatic–aromatic crosspeaks. GH8–GH8 crosspeaks are observed between each sequential 5′-G-*syn*–G-*anti*-3′ pair, as observed for other G-quadruplexes (9). Substitution of I^2 for G^2 results in a downfield shift of the H8 resonance on that nucleotide only and the appearance of an IH2 resonance at low field. Thus, comparison of the spectra allows unambiguous identification of the G^2H8. A G-quartet is shown in Fig. 4*B*. In the G-quartet structure, the IH2 will be near a GH8 resonance on a Hoogsteen-paired guanine and should give rise to an NOE crosspeak. This crosspeak is identified in the NOESY spectrum (Fig. 4*A*). Because the GH8 resonance had already been identified as G^{14}, this also identifies the relative location of the guanines in the G-quartet. Similar results and NOEs were observed for sequences I6 (I^6H2–$G^{10}H8$) and I11 ($I^{11}H2$–G^5H8), thus confirming the G-quartet structure and the hydrogen-bonding partners of each base in the two G-quartets.

The other aptamer derivatives were used to unambiguously identify the remaining bases. Sequence I8 confirmed the loop assignments for T^7, G^8, and T^9. Sequence A3 confirmed nonexchangeable assignments of T^3, T^4, T^{12}, and T^{13}, and sequence U4 was used to confirm the imino-proton-resonance assignments of T^4 and T^{13}. The sequence U4 derivative also increased resolution between imino resonances from nt 4 and 13, thus allowing unambiguous identification of an imino–imino NOE between these nucleotides. This result indicated that T^4 and T^{13} are probably base-paired.

The Quadruplex Is Unimolecular. Only 15 sets of nucleotide resonances are present, indicating that the quadruplex structure is either unimolecular or a symmetrical dimer or tetramer. Of the many possible quadruplexes that might form, only the two structures, a monomer and dimer, which are shown schematically in Fig. 5*B*, are consistent with the assignments of the G-quartets and the nonsequential NOE crosspeaks between G^2 and T^4 and between G^{11} and T^{13} (Figs. 3 and 4). The symmetry of the two strands in the potential dimeric structure (Fig. 5*B*) would not allow for the distinction of inter- vs. intramolecular NOEs. To break the symmetry of this potential hairpin dimer, an NMR sample containing a mixture of sequences I2 and I8 was made. The sample was heated to 90°C and slowly cooled to guarantee strand exchange between any potential preformed dimers. The

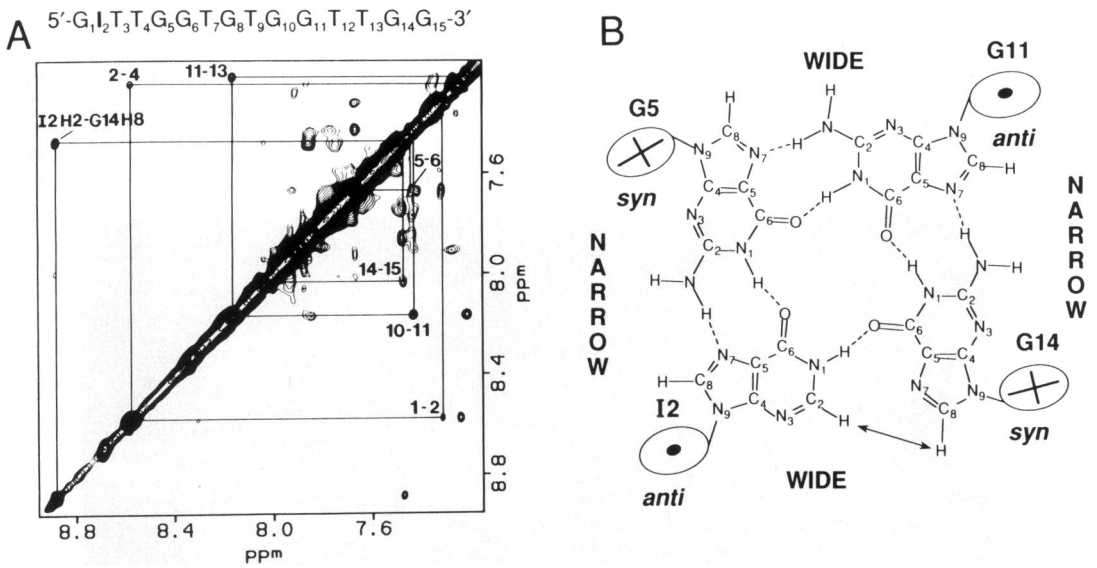

FIG. 4. (*A*) Region of NOESY spectrum of sequence I2 showing the base–base crosspeaks. Experimental conditions are the same as for Fig. 3 except 2mM strand concentration at 10°C and τ_m = 320 msec. Base–base connectivities observed between sequential 5′-*syn*–*anti*-3′ pairs are indicated by solid lines in lower right. Nonsequential connectivities (G^2–T^4 and G^{11}–T^{13}) are indicated by solid lines in upper left. Corresponding connectivities are observed for the thrombin aptamer and the other derivatives. The crosspeak between I^2H2 and $G^{14}H8$ is indicated. (*B*) Second quartet in the aptamer structure. The quartet containing I^2 is illustrated. The I^2H2 to $G^{14}H8$ connectivity is indicated by the arrow.

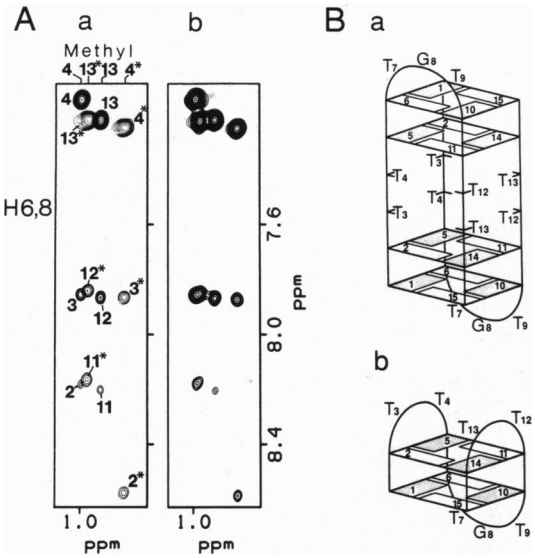

FIG. 5. (*A*) Portion of NOESY spectra (τ_m = 320 msec) in ^2H_2O showing some of the methyl-base crosspeaks at 10°C of sequences I8 and I2 (superimposed spectra of individual samples) (*a*) and a mixture of I8 and I2 (*b*). In *a* the I8 crosspeaks are indicated by the darker contours, and the I2 crosspeaks have the lighter contours and are labeled with *. Both samples contained 2 mM DNA/110 mM KCl, pH 6.1. The sample in *b* is a mixture of I8 and I2 at 1.6 mM I8/2.0 mM I2/110 mM KCl, pH 6.1. Spectra were acquired and processed as for Fig. 3. (*B*) Schematic models for the dimer (*a*) and monomer (*b*) structures of the thrombin aptamer that satisfy the connectivities determined by analysis of the NMR spectra from the derivatives. *Syn* nt are shaded. All other loop orientations for a monomer or dimer (and tetramers) were eliminated on the basis of the NMR data. The correct structure is the monomer (*b*).

NOESY spectrum of the mixture is essentially identical to the sum of NOESY spectra taken individually on sequences I2 and I8, and there are none of the additional shifted crosspeaks that would be expected if I2–I8 heterodimers had formed (Fig. 5*A* and regions not shown). It is theoretically possible that in the region shown a heterodimer of I8 and I2 would not shift the position of any of the crosspeaks—i.e., a change at one end of the molecule would not affect the other end of the molecule. However, this possibility is eliminated by examination of other regions of the spectrum and comparison to the chemical shifts of the thrombin aptamer. In an I2–I8 heterodimer, both inosines would be at one end of the dimer, and the other end would look like the parent dimer. Some crosspeaks in the parent aptamer spectra (e.g., G^8H8–G^8H1') are at different chemical shifts from those in the spectra of either I8 (I^8H8–I^8H1') or sequence I2 alone. None of these distinctive crosspeaks are seen in the spectrum of the mixture of sequences I2 and I8. The concentration independence of the optically A_{276} and DSC-determined t_m values (J.A.R., unpublished data) also indicates that the thrombin aptamer forms a unimolecular quadruplex.

Structural Features of the Thrombin Aptamer. The structural features of the thrombin aptamer are illustrated schematically in Figs. 4*B* and 5*B*(*b*) and in the molecular model in Fig. 6. The nucleotides in the two G-quartets are *5′-syn–anti-3′* along each "strand." Adjacent "strands" are antiparallel, resulting in G-quartets in which the bases are alternately *syn* and *anti* around the quartet, and there are two wide and two narrow grooves. The two G-quartets are connected by two TT loops that span the narrow grooves at one end and a TGT loop that spans one of the wide grooves at the other end of the quadruplex. This structure is thus significantly different from the solution structure of $d(G_4T_4G_4)$, which forms a dimeric quadruplex with one TTTT loop across the diagonal of each end G-quartet, resulting in one narrow, one wide, and two medium grooves, adjacent parallel and antiparallel strands, and *syn–syn–anti–anti* nt around each quartet (9). This structure also differs from the crystal structure of $d(G_4T_4G_4)$, which has the same quartet structure as the aptamer but has TTTT loops that span a wide groove at each end of the quadruplex (26) and from the tetramolecular parallel stranded G-quadruplexes, in which all bases are *anti* (28–30). The molecular model of the thrombin aptamer (Fig. 6), generated using metric matrix-distance geometry with NOE constraints and refined with X-PLOR (17), shows the overall conformation and orientation of the loops. An interesting feature is the probable formation of a T^4·T^{13} bp across the G-quartet. NMR evidence for the T^4·T^{13} bp includes a NOE between the imino protons of these bases. There is also a NOE between the T^4 and G^5 and the T^{13} and G^{14} imino resonances, indicating that this T·T bp stacks well on the top G-quartet. The calculated structure has a T^4·T^{13} bp hydrogen-bonded via the O4 carbonyl and N3 imino proton of each base; however, an alternate base pair hydrogen-bonded at O2 and N3 cannot be distinguished from the NMR data. The two base-paired thymines were invariant in all of the thrombin aptamers that were cloned, whereas T^3 and T^{12} were variable (6). Thus, all of the invariant bases in the aptamer sequence are involved in base pairs. In the consensus sequence, the nucleotides that span the wide groove are variable from 2–5 nt, indicating that 2 nt may be sufficient to span the wide groove. Interestingly, when there were only 2 nt the sequence was always GA (6).

Summary. These results show that it is possible to form an intramolecular DNA quadruplex with only two G-quartets

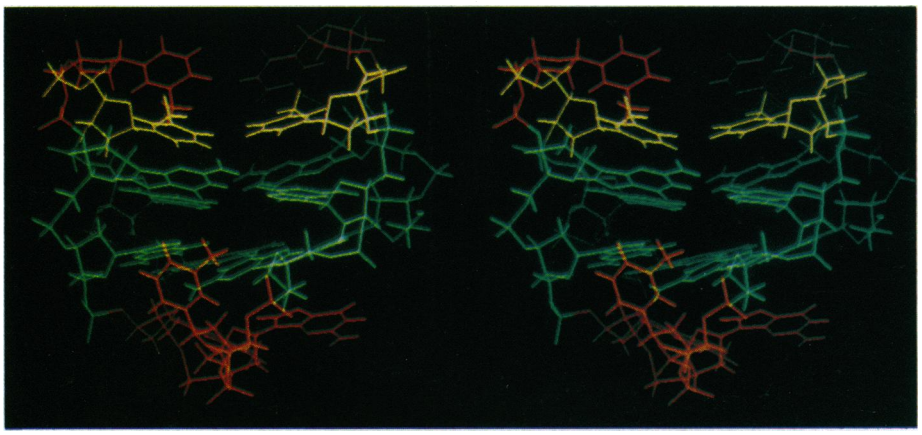

FIG. 6. Stereoview of a preliminary structure of the thrombin aptamer; a view into the wide groove is shown. In addition to the two G-quartets (green), a T^4·T^{13} bp (yellow) appears in this structure. G^8 and T^9 stack well on the bottom quartet, while T^7 is in the major groove.

and that a TT loop is sufficient to span the narrow groove, whereas a TGT loop (or possibly GA) is sufficient to span the wide groove. This result probably represents the minimal intramolecular G-quadruplex in the growing family of G-quadruplexes (9, 19, 26, 28–30). The three-dimensional structure provides a rationale for the consensus sequence of the thrombin-binding aptamers in that only the unpaired bases in the loops are variable. The unimolecular structure of this quadruplex aptamer is consistent with binding studies that favored a thrombin–aptamer stoichiometry of 1:1 (6). Because formation of a unimolecular structure is not concentration dependent, this is likely the relevant ligand structure for thrombin-binding. The elucidation of this structure should now allow for a rational design approach to increasing the stability and, perhaps, efficacy of this potential antithrombotic drug. In this regard, we note the structural similarity between hematin, which also inhibits thrombin (31–33), and the G-quartet.

We thank Karl Koshlap and Shiva Malek for synthesis and purification of DNA. This work was supported by grants from the National Institutes of Health (R01 GM 37254-06 and R01 GM48123-01) and by National Science Foundation Presidential Young Investigator Award (DMB 89-58280) with matching funds from Amgen, Inc., Monsanto Co., and Sterling Winthrop Drug, Inc., to J.F.; and by National Institutes of Health Predoctoral Fellowships to R.F.M. and F.W.S.

1. Ellington, A. D. & Szostak, J. W. (1990) *Nature (London)* **346,** 818–822.
2. Szostak, J. W. (1992) *Trends Biochem. Sci.* **17,** 89–93.
3. Tuerk, C. & Gold, L. (1990) *Science* **249,** 505–510.
4. Irvine, D., Tuerk, C. & Gold, L. (1991) *J. Mol. Biol.* **222,** 739–761.
5. Innis, M. A., Myambo, K. B., Gelfand, D. H. & Brow, M. A. D. (1988) *Proc. Natl. Acad. Sci. USA* **85,** 9436–9440.
6. Bock, L. C., Griffin, L. C., Latham, J. A., Vermaas, E. H. & Toole, J. J. (1992) *Nature (London)* **355,** 564–566.
7. Tuerk, C., MacDougal, S. & Gold, L. (1992) *Proc. Natl. Acad. Sci. USA* **89,** 6988–6992.
8. Guschlbauer, W., Chantot, J.-F. & Thiele, D. (1990) *J. Biomol. Struct. Dyn.* **8,** 491–511.
9. Smith, F. W. & Feigon, J. (1992) *Nature (London)* **356,** 164–168.
10. Feigon, J., Sklenar, V., Wang, E., Gilbert, D. E., Macaya, R. F. & Schultze, P. (1992) *Methods Enzymol.* **211,** 235–253.
11. Sklenar, V. & Bax, A. (1987) *J. Magn. Reson.* **74,** 469–479.
12. States, D. J., Haberkorn, R. A. & Ruben, D. J. (1982) *J. Magn. Reson.* **48,** 286–292.
13. Kumar, A., Ernst, R. R. & Wüthrich, K. (1980) *Biochem. Biophys. Res. Commun.* **95,** 1–6.
14. Marion, D. & Bax, A. (1988) *J. Magn. Reson.* **80,** 528–533.
15. Davis, D. G. & Bax, A. (1985) *J. Am. Chem. Soc.* **107,** 2820–2821.
16. Wüthrich, K. (1986) *NMR of Proteins and Nucleic Acids* (Wiley, New York).
17. Brünger, A. T. (1992) X-PLOR Manual (Yale Univ., New Haven, CT), Version 3.0.
18. Yip, P. & Case, D. A. (1989) *J Magn. Reson.* **83,** 643–648.
19. Wang, Y., de los Santos, C., Gao, X., Greene, K., Live, D. & Patel, D. J. (1991) *J. Mol. Biol.* **222,** 819–832.
20. Jin, R., Breslauer, K. J., Jones, R. A. & Gaffney, B. L. (1990) *Science* **250,** 543–546.
21. Hardin, C. C., Henderson, E., Watson, T. & Prosser, J. K. (1991) *Biochemistry* **30,** 4460–4472.
22. Sen, D. & Gilbert, W. (1990) *Nature (London)* **344,** 410–414.
23. Williamson, J. R., Raghuraman, M. K. & Cech, T. R. (1989) *Cell* **59,** 871–880.
24. Sundquist, W. I. & Klug, A. (1989) *Nature (London)* **342,** 825–829.
25. Pinnavaia, T. J., Marshall, C. L., Metterl, C. M., Fisk, C. L., Miles, T. & Becker, E. D. (1978) *J. Am. Chem. Soc.* **100,** 3625–3627.
26. Kang, C., Zhang, X., Ratliff, R., Moyzis, R. & Rich, A. (1992) *Nature (London)* **356,** 126–131.
27. Wang, Y., Jin, R., Gaffney, B., Jones, R. A. & Breslauer, K. J. (1991) *Nucleic Acids Res.* **19,** 4619–4622.
28. Wang, Y. & Patel, D. J. (1992) *Biochemistry* **31,** 8112–8119.
29. Cheong, C. & Moore, P. B. (1992) *Biochemistry* **31,** 8406–8414.
30. Jin, R., Gaffney, B. L., Wang, C., Jones, R. A. & Breslauer, K. J. (1992) *Proc. Natl. Acad. Sci. USA* **89,** 8832–8836.
31. Jones, R. L. (1986) *J. Exp. Med.* **163,** 724–739.
32. Glueck, R., Green, D., Cohen, I. & Ts'ao, C.-H. (1983) *Blood* **61,** 243–249.
33. Green, D., Reynolds, N., Klein, J., Kohl, H. & Ts'ao, C.-H. (1983) *J. Lab. Clin. Med.* **102,** 361–369.